福島県立医科大学 学術機関リポジトリ

FUKUSHIMA MEDICAL UNIVERSITY

Title	Ectopic expression of a tight-junction molecule in podocytes is associated with childhood onset nephrotic syndrome(本文)
Author(s)	菅野, 修人
Citation	
Issue Date	2017-03-24
URL	http://ir.fmu.ac.jp/dspace/handle/123456789/956
Rights	This is the pre-peer reviewed version. Published version "Pediatr Res. 2019 Oct;86(4):485-491. doi: 10.1038/s41390-019-0423-7. © 2019, Springer Nature"
DOI	
Text Version	ETD

This document is downloaded at: 2024-04-25T11:40:49Z

Fukushima Medical University

学　位　論　文

Ectopic expression of a tight-junction molecule in podocytes is associated with childhood onset nephrotic syndrome

(ポドサイトにおけるタイト結合分子の異所性発現は小児ネフローゼ症候群に関連している)

医学研究科 (平成 25 年度入学)　小児科学分野

学籍番号　135010

菅野　修人

福島県立医科大学小児科学講座

【略語】

AR: after remission (寛解後)
BR: before remission (寛解前)
BSA: bovine serum albumin (ウシ血清アルブミン)
CLDN: Claudin (クローディン)
FSGS: focal segmental glomerulosclerosis (巣状分節性糸球体硬化症)
HSPG: Heparan Sulfate Proteoglycan (ヘパラン硫酸プロテオグリカン)
IgA-N: IgA nephritis (IgA 腎症)
mAb: monoclonal antibody (モノクローナル抗体)
MCD: minimal change disease (微小変化群)
NS: Nephrotic syndrome (ネフローゼ症候群)
pAb: polyclonal antibody (ポリクローナル抗体)
PBS: phosphate-buffered saline (リン酸緩衝生理食塩水)
PECs: parietal epithelial cells (壁側上皮細胞)
SDs: slit diaphragms (スリット膜)
TJs: tight junctions (タイト結合)

【Introduction】

Nephrotic syndrome (NS) is a complex disorder characterized by severe proteinuria along with hypoalbuminemia, edema and hyperlipidemia. The primary NS in children is most frequently caused by minimal change disease (MCD) and focal segmental glomerulosclerosis (FSGS). In both diseases, podocyte injury initiates foot process effacement, whereas the change in podocyte morphology and the resulting proteinuria are usually reversible and irreversible in MCD and FSGS, respectively. However, the pathogenesis of these diseases remains obscure, and the majority of cases cannot be explained by mutations in various podocyte genes (1, 2). In addition, it is unresolved whether MCD and FSGS are distinct types of one disease or two different diseases (3).

During early stage of glomerulogenesis, immature podocytes represent columnar epithelia with tight junctions (TJs) (4, 5, 6). On the other hand, mature podocytes lack TJs and form slit diaphragms (SDs) between opposing foot processes, establishing the final barrier to urinary protein loss. Interestingly, in several animal models for NS, TJ-like structures are generated in instead of decreased or disappeared SDs (7, 8, 9, 10). The SD-TJ transition is also observed in human MCD cases (11). Nevertheless, it is indefinite by which mechanism the SD-TJ transition occurs in both MCD and FSGS.

Claudins (CLDNs) are capable of forming TJ strands (12) and thereby the backbone of TJs. The CLDN family consists of 27 members in mammals, and shows distinct expression patterns in tissue- and cell-type specific manners (13, 14, 15, 16). Among CLDNs expressed in normal renal corpuscle, CLDN1 and CLDN2 are known to be observed in parietal epithelial cells (PECs), which cover the inner surface of Bowman's capsule, but not in podocytes (17, 18, 19). During the SD-TJ transition in MCD and FSGS, however, it is unknown which CLDN subtype is responsible for newly formed TJs in injured podocytes.

On the other hand, CLDN2 is also detected in epithelial cells of the proximal tubule and the thin descending limb of Henle along the normal renal tubule (17). CLDN2 is one of the pore-forming CLDNs, and in the proximal tubule, it has a role in the bulk reabsorption of salt and water (20). Therefore, I focused on CLDN2 and found that ectopic expression of CLDN2 existed in glomeruli of primary NS. In the present study, I show ectopic expression of CLDN2 in podocytes of pediatric MCD and FSGS. I also demonstrate that CLDN2 is associated with their pathogenesis, suggesting that both diseases are "the CLDN2-related podocytopathies". Moreover, I discuss the possible mechanism by which CLDN2 expression in podocytes lead to their dysfunction.

【Methods】

Patients

Renal frozen specimens were obtained by needle biopsy from 49 pediatric patients: 21 subjects (8 subjects before remission [BR] and 13 after remission [AR]) with MCD, 18 (8 BR and 10 AR) with FSGS, and 10 with IgA nephritis (IgA-N) as disease controls. This study was approved by the Ethical Committee of Fukushima Medical University (approval number: 1809).

Clinical data for the subjects were documented at the time of biopsy, and were summarized in Tables 1 and 2. Proteinuria and urinary occult blood were semi-quantitatively scored as follows: (−)=0, (±)=0.5, (1+)=1, (2+)=2, (3+)=3, and (4+)=4.

Antibodies

Rabbit polyclonal antibody (pAb) against CLDN2 was the gift from Dr. Furuse (National Institute for Physiological Sciences, National Institutes of Natural Sciences) (21). Rabbit pAbs against CLDN1 and podocin were purchased from IBL (Gunma, Japan) and SIGMA (St. Louis, MO, USA), respectively. Mouse monoclonal antibodies (mAbs) against CD34 (clone NU-4A1), podocalyxin (clone #222328) and synaptopodin (clone G1D4) were obtained from Nichirei Bioscience (Tokyo, Japan), R&D Systems (Minneapolis, MN, USA) and Progen Biotechnik (Heidelberg Germany), respectively. A rat anti-Heparan Sulfate Proteoglycan (HSPG) (Perlecan) mAb (clone A7L6) was purchased from Merck Millipore (Temecula, CA, USA). The secondary antibodies used were as follows: AlexaFluor488-labeled donkey anti-rabbit IgG (H+L) (Invitrogen, Waltham, MA, USA), Cy3-conjugated AffiniPure donkey anti-mouse IgG (H+L) (Jackson ImmunoResearch, West Grove, PA, USA), AlexaFluor647-labeled AffiniPure donkey anti-rat IgG (H+L) (Jackson ImmunoResearch) and immunogold conjugate EM goat anti-rabbit IgG (BBI Solutions, Cardiff, UK).

Immunohistochemistry

Renal biopsy specimens were frozen on dry ice and kept at −80°C until use. They were sectioned at a thickness of 5 μm and fixed in ice-cold methanol for 15 min at −20°C. After washing with phosphate-buffered saline (PBS), sections were blocked in 2% bovine serum albumin (BSA) for 1 h at room temperature. After washing, they were subsequently incubated with primary antibodies overnight at 4°C and rinsed again with PBS followed by a reaction for 1 h at room temperature with appropriate secondary antibodies. They were then mounted after washing with PBS. All samples were

examined using a laser-scanning confocal microscopy (FV1000, OLYMPUS, Tokyo, Japan).

Calculations

The CLDN2-positive area was calculated using image processing software (ImageJ, Java). The images stained with CLDN2 and HSPG (Perlecan) were set the threshold from 100 to 255, in order to exclude background signals. A circle was drawn by free hand along the inside of PECs, and the total area in the circle (A) and the CLDN2-expression area in the circle (B) were determined. The CLDN2-positive area was defined as B/A × 100 (%), and represented using box-and-whisker plots.

Immunoelectron microscopy

Renal biopsy tissues were fixed with periodate-lysine-paraformaldehyde for 2 h at 4°C, and, after washing with PBS, they were incubated with polyvinylpyrrolidone-sucrose overnight at 4°C. They were then frozen by liquid nitrogen and ultrathin cryosections were prepared using a Leica Ultracut UCT microtome equipped with the FCS cryoattachment (Wien, Austria) at −20°C. They were transferred to nickel grids (150 mesh) with coating in formvar and carbon, and subsequent incubation steps were carried out by floating grids on droplets of the filtered soluction. After quenching free aldehyde groups with PBS/0.01 M glycine, sections were incubated with rabbit anti-CLDN2 pAb overnight at 4°C, and reacted for 1 h at room temperature with 10 nm gold-labeled goat anti-rabbit IgG followed by a fixation with 2.5% glutaraldehyde buffered with 0.1 M PBS (pH 7.4). They were subsequently contrasted with 3% uranyl acetate solution for 40 min, and absorption-stained with 3% polyvinyl alcohol containing 0.2% acidic uranyl acetate for 40 min. Micrographs were captured using an electron microscope (JEM1230, JOEL).

Statistical analysis

All values are shown as the mean ± standard deviation (SD) except for those of the CLDN2-positive area. Statistical analysis was performed by IBM SPSS statistics 23 software (Chicago, IL, USA). Results were analyzed using two-sample *t*-test and one way analysis of variance (ANOVA).

163 【Results】

164 **CLDN2 is ectopically detected in MCD and FSGS glomeruli**

165 I first examined, by immunohistochemistry, the expression of CLDN2 in glomeruli
166 obtained from pediatric MCD and FSGS patients, as well as in those from IgA-N
167 subjects as disease controls. To distinguish the overall structure of glomeruli, the
168 endothelial marker CD34 and the basement membrane marker HSPG (Perlecan) were
169 co-immunostained with CLDN2. As shown in Figure 1, strong filamentous signals for
170 CLDN2 appeared to be detected in the before remission cases with MCD and FSGS, but
171 not in subjects with IgA-N. CLDN2 was also occasionally observed within whole cell
172 bodies. These CLDN2 signals were generally distributed close to the basement
173 membrane and separated from endothelial cells, implying that CLDN2-expressing cells
174 correspond to podocytes. By contrast, in the after remission cases with the MCD and
175 FSGS, the CLDN2 expression was strikingly decreased, and the filamentous and
176 cytoplasmic staining disappeared.

177 I also quantitatively evaluated the CLDN2 expression by calculating the positive area
178 in glomeruli (Figure 2). The CLDN2-stained region in MCD and FSGS glomeruli
179 before remission was significantly greater than that after remission and in IgA-N
180 patients. In addition, the abundance of CLDN2 expression was well correlated with the
181 amounts of proteinuria of each group at the time of biopsy (Table 1 and 2). Interestingly,
182 among before remission subjects, CLDN2 was expressed in MCD glomeruli at high
183 levels compared with that in FSGS.

184

185 **CLDN2 is expressed in MCD and FSGS podocytes**

186 To determine whether CLDN2-expressing cells represent podocytes, I next performed
187 multiple immunostaining using the podocyte markers synaptopodin (SYNPO) and
188 podocalyxin (PODXL) (22, 23) (Figure 3). In both MCD and FSGS glomeruli before
189 remission, CLDN2 was at least in part colocalized with SYNPO and PODXL,
190 suggesting that CLDN2 expression is observed in podocytes.

191 I subsequently verified, by immunogold immunoelectron microscopy, the nature of
192 CLDN2-positve cells in MCD glomeruli before remission, as well as the detailed
193 subcellular localization of CLDN2 (Figure 4). The CLDN2 labeling was detected not
194 only in residual foot processes of podocytes (Figure 4A) but also in fused foot processes
195 (Figure 4B). Importantly, CLDN2 was also concentrated along newly formed TJs in
196 podocytes (Figure 4C).

197

198 **CLDN1 is not expressed in MCD glomeruli but segmentally observed in FSGS**

199 I also evaluated the CLDN1 expression in renal corpuscle of MCD and FSGS cases
200 before remission (Figure 5). As expected, PECs were positive for CLDN1 in both
201 diseases. By contrast, in glomeruli, the CLDN1 signals were not apparently detected for
202 MCD subjects. In addition, CLDN1 was only focally and segmentally expressed in
203 FSGS glomeruli with a trabecular pattern.
204
205 **Newly formed TJs constructed by CLDN2 are generated together with decrease of**
206 **SDs in MCD and FSGS glomeruli before remission**
207 To confirm the SD-TJ transition, I performed multiple immunostaining using the SDs
208 marker podocin (24), and compared CLDN2 and podocin expression in MCD and FSGS
209 glomeruli (Figure 6). In the before remission cases with MCD and FSGS, the
210 filamentous signals for podocin were decreased and changed to the granulated signals
211 together with the expression of strong filamentous signals for CLDN2. By contrast, in
212 the after remission cases with MCD and FSGS, the filamentous signals for podocin
213 were recovered together with decreased expression for CLDN2.
214

【Discussion】

In the present study, I found that CLDN2, which is detected in epithelial cells of Bowman's capsule, the proximal tubule and the thin descending limb of Henle along the normal nephron (17), was ectopically expressed on injured podocytes in pediatric MCD and FSGS. In both diseases, CLDN2 was distributed along the glomerular basement membrane maker HSPG, and apart from the vascular endothelial marker CD34. In addition, CLDN2 was at least in part colocalized with the podocyte markers SYNPO and PODXL in MCD and FSGS. Moreover, CLDN2-immunogold signals was observed in podocytes, especially in residual and fused foot processes as well as at TJs, definitively indicating that CLDN2-expressing cells represent podocytes. Hence, immunofluorescence and immunoelectron studies for CLDN2 appear to be a powerful tool for diagnosis of these primary NS. Since no substantial abnormality in glomerular structure is detected in MCD by light microcopy, CLDN2 should be a novel diagnostic marker especially for these patients who are resistant to steroid therapy and underwent renal biopsy (25).

Although both MCD and FSGS are typical podocyte diseases (26, 27), information on the pathophysiological basis for these diseases is still fragmentary. In this regard, it is noteworthy that ectopic expression of CLDN2 on podocytes was observed not only in MCD but also in FSGS as far as we determined. Thus, both MCD and FSGS could be regarded as "the CLDN2-related podocytopathies". Lower expression levels of CLDN2 in FSGS before remission compared with that in MCD most probably reflect podocyte loss in FSGS. The CLDN2-immunoreactive area in podocytes of both diseases after remission was significantly decreased to levels similar to that of the disease control group, further supporting that the CLDN2 expression is involved in their pathogenesis. Since circulating glomerular permeability factors, including angiopoietin-like-4 and urokinase plasminogen activator receptor in MCD and FSGS, respectively, are expected to result in the onset of these diseases (3, 28, 29, 30), it is intriguing to elucidate whether and how these factors are associated with the CLDN2 expression in damaged podocytes.

The CLDN1 expression, which is restricted in PECs along the healthy nephron (17, 18), is induced in glomerulus from humans and animals with diabetic nephropathy (31). On the other hand, we demonstrated that CLDN1 was not principally observed in glomerular tuft of pediatric MCD. In FSGS glomeruli before remission, the CLDN1 signals displayed a cord-like array in focal and segmental patterns, which are totally different from those of CLDN2. In FSGS, PECs are activated on Bowman's capsule and migrate onto the glomerular capillary to substitute or dislocate podocytes (32).

Activated PECs in glomerulosclerotic lesions are also known to positive for CLDN1 (33). Taken collectively, CLDN1-expressing cells in glomeruli of our FSCG cases may correspond to activated PECs.

Podocin is one of the proteins forming SDs, and its mutations (NPHS2 gene) are responsible for the autosomal recessive form of steroid-resistant NS (24). The strong filamentous signals for CLDN2 were appeared together with decrease of the filamentous signals and change to the granulated pattern for podocin in the before remission cases with MCD and FSGS. These changes are suggested that SDs are displaced to TJs constructed by CLDN2 in the before remission cases of MCD and FSGS. In the after remission cases with MCD and FSGS, the filamentous signals for podocin were recovered. It is seemed that the SDs related molecules containing podocin accumulate and form SDs again.

Several TJ proteins such as junctional adhesion molecule-A, coxsackie and adenovirus receptor, ZO-1 and cingulin, are concentrated at the SD in mature podocytes (34, 35, 36). Among them, ZO-1 is indispensable for the interdigitation of foot processes and the formation of SDs (37), even though the precise role of other TJ components in glomerular filtration barrier remains elusive. Therefore, I speculate that the ectopically expressed CLDN2 could recruit these TJ constituents from the SD pool and disrupt the architecture of foot processes and SDs, resulting in being dedifferentiated into immature podocytes with glomerular dysfunction. To prove this idea, CLDN2-knockin mice, in which CLDN2 is podocyte-specifically expressed under human podocin promoter, were generated, and their characterization is under analysis (Ichikawa-Tomikawa et al., unpublished data).

In conclusion, I showed that both MCD and FSGS in children possessed the same pathological findings in terms of ectopic CLDN2 expression on podocytes. I also demonstrated that the abundance of CLDN2 was diminished after remission, indicating that the levels of CLDN2 expression are related to the disease state. Further studies are required to clarify the functional relevance of CLDN2 expression in the pathogenesis of these diseases.

【Acknowledgments】

I thank Prof. M Hosoya, assistant Prof. Y Kawasaki, and Prof. H Chiba (Fukushima Medical University) for their advice. I am also grateful to Drs. N Ichikawa-Tomikawa and M Mizuko (Fukushima Medical University) for immunohistochemical study; Dr. K Sugimoto (Fukushima Medical University) for preparing figures; and Dr. H Kurihara (Juntendo University) for immunoelectron microscopy analysis.

288 【**References**】

289 1. Allison A Eddy, Jordan M Symons: Nephrotic syndrome in childhood. Lancet 362:
290 629-639, 2003

291 2. D'Agati VD, Kaskel FJ, Falk RJ: Focal segmental glomerulosclerosis. N Engl J Med.
292 365: 2398-2411, 2011

293 3. Floege J, Amann K: Primary glomerulonephritides. Lancet 387: 2036-2048, 2016

294 4. Reeves W, Caulfield JP, Farquhar MG: Differentiation of epithelial foot processes
295 and filtration slits: sequential appearance of occluding junctions, epithelial
296 polyanion, and slit membranes in developing glomeruli. Lab Invest. 39: 90-100,
297 1978

298 5. Grahammer F, Schell C, Huber TB: The podocyte slit diaphragm—from a thin grey
299 line to a complex signalling hub. Nat Rev Nephrol. 9: 587-598, 2013

300 6. Schell C, Wanner N, Huber TB: Glomerular development—shaping the
301 multi-cellular filtration unit. Semin Cell Dev Biol. 36: 39-49, 2014

302 7. Pricam C, Humbert F, Perrelet A, Amherdt M, Orci L: Intercellular junctions in
303 podocytes of the nephrotic glomerulus as seen with freeze-fracture. Lab Invest. 33:
304 209-218, 1975

305 8. Ryan GB, Leventhal M, Karnovsky MJ: A freeze-fracture study of the junctions
306 between glomerular epithelial cells in aminonucleoside nephrosis. Lab Invest. 32:
307 397-403, 1975

308 9. Caulfield JP, Reid JJ, Farquhar MG: Alterations of the glomerular epithelium in
309 acute aminonucleoside nephrosis. Evidence for formation of occluding junctions
310 and epithelial cell detachment. Lab Invest. 34: 43-59, 1976

311 10. Kurihara H, Anderson JM, Kerjaschki D, Farquhar MG: The altered glomerular
312 filtration slits seen in puromycin aminonucleoside nephrosis and protamine
313 sulfate-treated rats contain the tight junction protein ZO-1. Am J Pathol. 141:
314 805-816, 1992

11. Lahdenkari AT, Lounatmaa K, Patrakka J, Holmberg C, Wartiovaara J, Kestilä M, Koskimies O, Jalanko H: Podocytes are firmly attached to glomerular basement membrane in kidneys with heavy proteinuria. J Am Soc Nephrol. 15: 2611-2618, 2004

12. Furuse M, Sasaki H, Fujimoto K, Tsukita S. A single gene product, claudin-1 or -2, reconstitutes tight junction strands and recruits occludin in fibroblasts. J Cell Biol.143: 391–401, 1998

13. Tsukita S, Furuse M, Itoh M. Multifunctional strands in tight junctions. Nat Rev Mol Cell Biol. 2: 285–293, 2001

14. Van Itallie CM, Anderson JM: Claudins and epithelial paracellular transport. Annu Rev Physiol. 68: 403-429, 2006

15. Chiba H, Osanai M, Murata M, Kojima T, Sawada N: Transmembrane proteins of tight junctions. Biochim Biophys Acta. 1778: 588-600, 2008

16. Günzel D, Yu AS: Claudins and the modulation of tight junction permeability. Physiol Rev. 93: 525-569, 2013

17. Kiuchi-Saishin Y, Gotoh S, Furuse M, Takasuga A, Tano Y, Tsukita S: Differential expression patterns of claudins, tight junction membrane proteins, in mouse nephron segments. J Am Soc Nephrol. 13: 875-886, 2002

18. Ohse T, Pippin JW, Vaughan MR, Brinkkoetter PT, Krofft RD, Shankland SJ: Establishment of conditionally immortalized mouse glomerular parietal epithelial cells in culture. J Am Soc Nephrol. 19: 1879-1890, 2008

19. Ohse T, Pippin JW, Chang AM, Krofft RD, Miner JH, Vaughan MR, Shankland SJ: The enigmatic parietal epithelial cell is finally getting noticed: a review. Kidney Int. 76: 1225-1238, 2009

20. Yu AS: Claudins and the kidney. J Am Soc Nephrol. 26: 11-19, 2015

341 21. Kubota K, Furuse M, Sasaki H, Sonoda N, Fujita K, Nagafuchi A, Tsukita S:
342 Ca^{2+}-independent cell-adhesion activity of claudins, a family of integral membrane
343 proteins localized at tight junctions. Curr Biol. 9: 1035-1038, 1999

344 22. Kerjaschki D, Sharkey DJ, Farquhar MG: Identification and characterization of
345 podocalyxin—the major sialoprotein of the renal glomerular epithelial cell. J Cell
346 Biol. 98: 1591-1596, 1984

347 23. Mundel P, Heid HW, Mundel TM, Krüger M, Reiser J, Kriz W: Synaptopodin: an
348 actin-associated protein in telencephalic dendrites and renal podocytes. J Cell Biol.
349 139: 193-204, 1997

350 24. Caridi G, Bertelli R, Carrea A, Di Duca M, Catarsi P, Artero M, Carraro M,
351 Zennaro C, Candiano G, Musante L, Seri M, Ginevri F, Perfumo F, Ghiggeri GM:
352 Prevalence, genetics, and clinical features of patients carrying podocin mutations in
353 steroid-resistant nonfamilial focal segmental glomerulosclerosis. J Am Soc Nephrol.
354 12: 2742-2746, 2001

355 25. Gulati S, Sharma AP, Sharma RK, Gupta A, Gupta RK: Do current
356 recommendations for kidney biopsy in nephrotic syndrome need modifications?
357 Pediatr Nephrol. 17: 404-408, 2002

358 26. Wiggins RC: The spectrum of podocytopathies: a unifying view of glomerular
359 diseases. Kidney Int. 71: 1205-1214, 2007

360 27. D'Agati VD: The spectrum of focal segmental glomerulosclerosis: new insights.
361 Curr Opin Nephrol Hypertens. 17: 271-281, 2008

362 28. Clement LC, Avila-Casado C, Macé C, Soria E, Bakker WW, Kersten S, Chugh SS:
363 Podocyte-secreted angiopoietin-like-4 mediates proteinuria in
364 glucocorticoid-sensitive nephrotic syndrome. Nat Med. 17: 117-122, 2011

365 29. Wei C, El Hindi S, Li J, Fornoni A, Goes N, Sageshima J, Maiguel D, Karumanchi
366 SA, Yap HK, Saleem M, Zhang Q, Nikolic B, Chaudhuri A, Daftarian P, Salido E,
367 Torres A, Salifu M, Sarwal MM, Schaefer F, Morath C, Schwenger V, Zeier M,
368 Gupta V, Roth D, Rastaldi MP, Burke G, Ruiz P, Reiser J: Circulating urokinase

369 receptor as a cause of focal segmental glomerulosclerosis. Nat Med. 17: 952-960,
370 2011

371 30. Chugh SS, Clement LC, Macé C: New insights into human minimal change disease:
372 lessons from animal models. Am J Kidney Dis. 59: 284-292, 2012

373 31. Hasegawa K, Wakino S, Simic P, Sakamaki Y, Minakuchi H, Fujimura K, Hosoya
374 K, Komatsu M, Kaneko Y, Kanda T, Kubota E, Tokuyama H, Hayashi K, Guarente
375 L, Itoh H: Renal tubular Sirt1 attenuates diabetic albuminuria by epigenetically
376 suppressing Claudin-1 overexpression in podocytes. Nat Med. 19: 1496-1504, 2013

377 32. Shankland SJ, Smeets B, Pippin JW, Moeller MJ: The emergence of the glomerular
378 parietal epithelial cell. Nat Rev Nephrol. 10: 158-173, 2014

379 33. Smeets B, Kuppe C, Sicking EM, Fuss A, Jirak P, van Kuppevelt TH, Endlich K,
380 Wetzels JF, Gröne HJ, Floege J, Moeller MJ: Parietal epithelial cells participate in
381 the formation of sclerotic lesions in focal segmental glomerulosclerosis. J Am Soc
382 Nephrol. 22: 1262-1274, 2011

383 34. Schnabel E, Anderson JM, Farquhar MG: The tight junction protein ZO-1 is
384 concentrated along slit diaphragms of the glomerular epithelium. J Cell Biol. 111:
385 1255-1263, 1990

386 35. Nagai M, Yaoita E, Yoshida Y, Kuwano R, Nameta M, Ohshiro K, Isome M,
387 Fujinaka H, Suzuki S, Suzuki J, Suzuki H, Yamamoto T: Coxsackievirus and
388 adenovirus receptor, a tight junction membrane protein, is expressed in glomerular
389 podocytes in the kidney. Lab Invest. 83: 901-911, 2003

390 36. Fukasawa H, Bornheimer S, Kudlicka K, Farquhar MG: Slit diaphragms contain
391 tight junction proteins. J Am Soc Nephrol. 20: 1491-1503, 2009

392 37. Itoh M, Nakadate K, Horibata Y, Matsusaka T, Xu J, Hunziker W, Sugimoto H: The
393 structural and functional organization of the podocyte filtration slits is regulated by
394 Tjp1/ZO-1. PLoS One 9: e106621, 2014

395

Table 1: Clinical characteristics of patients in this study.

	MCD	FSGS	*p* value[a]	IgA-N	*p* value[b]
Total number of patients	**21**	**18**		**10**	
Age at onset	**5.38±3.78**	**6.00±3.74**	**0.61**	**11.40±2.88**	**<0.01**
Age at biopsy	**7.05±4.01**	**8.17±4.69**	**0.43**	**12.80±2.90**	**<0.01**
Sex (male) (%)	**12 (57%)**	**16 (89%)**		**7 (70%)**	
Proteinuria (maximum)					
Urinary protein score	**3.50±0.95**	**3.75±0.45**	**0.31**	**1.50±1.05**	**<0.01**
Proteinuria (g/day)	**4.49±4.13**	**10.17±6.46**	**<0.01**	**0.49±0.81**	**<0.01**
Urine occult blood score	**0.21±0.68**	**0.39±0.96**	**0.51**	**1.95±1.12**	**<0.01**
Serum creatinine (mg/dl)	**0.32±0.09**	**0.44±0.21**	**<0.05**	**0.54±0.14**	**<0.01**

The values represent the mean ±SD.

[a, b]: Two-sample *t*-test.

[a]: *p* value compared the values in the MCD group with those in the FSGS group.

[b]: *p* value compared the values in the MCD group with those in the IgA-N group.

Table 2: Comparison of clinical characteristics between the before and after remission cases in patients with MCD and FSGS.

	MCD			FSGS		
	BR	AR	*p* value[a]	BR	AR	*p* value[b]
Total number of patients	8	13		8	10	
Age at onset	7.50±4.24	4.07±2.91	<0.05	6.25±3.58	5.80±4.05	0.81
Age at biopsy	7.63±4.10	6.69±4.07	0.62	6.88±3.80	9.20±5.27	0.31
Sex (male) (%)	2 (25%)	10 (77%)		6 (75%)	10 (100%)	
Proteinuria						
(At the time of biopsy)						
Urinary protein score	2.75±1.04	0.04±0.14	<0.01	2.81±1.46	0.00±0.00	<0.01
Proteinuria (g/day)	2.14±1.46	0.01±0.03	<0.01	1.88±1.47	0.00±0.01	<0.01
(maximum)						
Urinary protein score	3.50±0.93	3.50±1.00	1.00	3.75±0.46	3.75±0.46	1.00
Proteinuria (g/day)	4.06±2.31	4.77±5.08	0.72	7.79±7.13	12.88±4.68	0.13
Urine occult blood score	0.56±1.05	0.00±0.00	0.17	0.81±1.36	0.05±0.16	0.16
Serum creatinine (mg/dl)	0.33±0.12	0.32±0.08	0.87	0.38±0.22	0.49±0.20	0.30

BR: before remission, AR: after remission. The values represent the mean ±SD.

[a, b]: Two-sample *t*-test.

[a]: *p* value compared the values in the BR group with those in the AR group of MCD.

[b]: *p* value compared the values in the BR group with those in the AR group of FSGS.

441

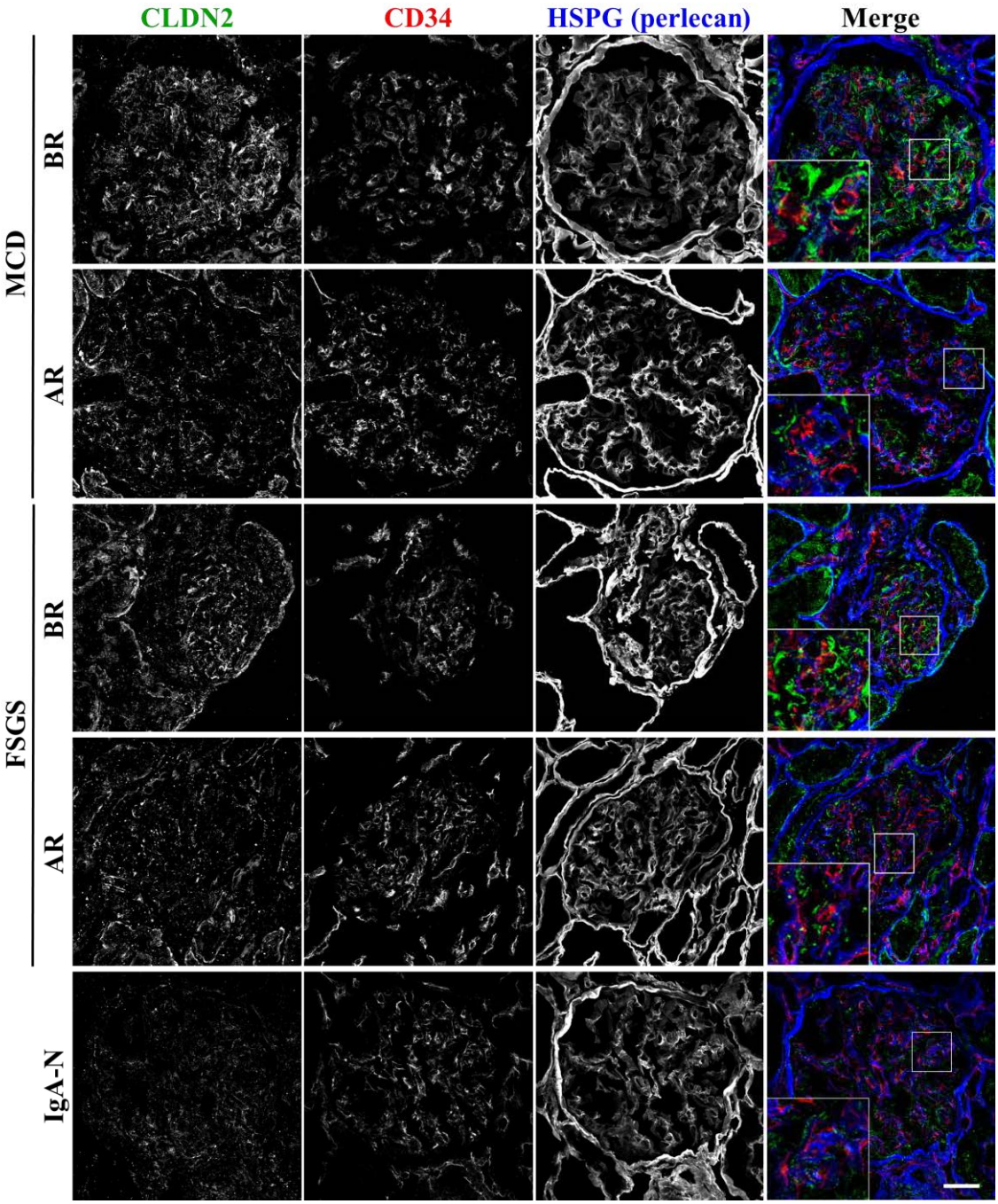

442

443 **Figure 1:** CLDN2 is ectopically expressed in MCD and FSGS glomeruli.

444 Renal biopsy sections were subjected to immunostaining with the corresponding
445 antibodies. Typical micrographs are shown for the before remission (BR) and after
446 remission (AR) cases in MCD and FSGS, as well as the case in IgA-N. In the Merge
447 panels, CLDN2 is stained green, CD34 is red and HSPG (perlecan) is blue. Bar, 50 μm.

448

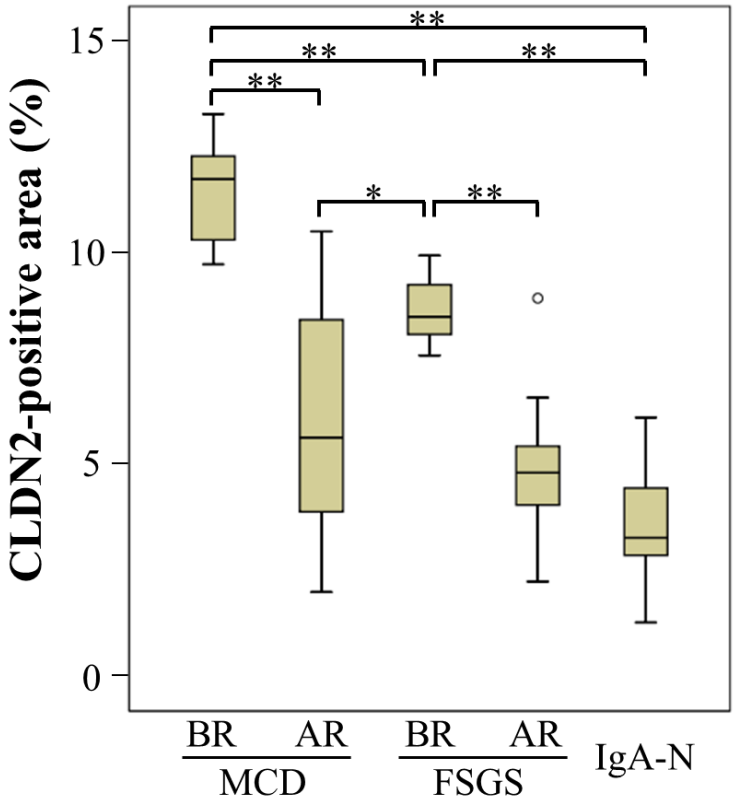

Figure 2: The CLDN2-positive area is increased in MCD and FSGS glomeruli.

Data are represented using box-and-whisker plots for cases before remission (BR; n=8) and after remission (AR; n=13) with MCD, subjects BR (n=8) and AR (n=10) with FSGS, and IgA-N cases (n=10). Results are analyzed using one way ANOVA. *: $p < 0.05$, and **: $p < 0.01$.

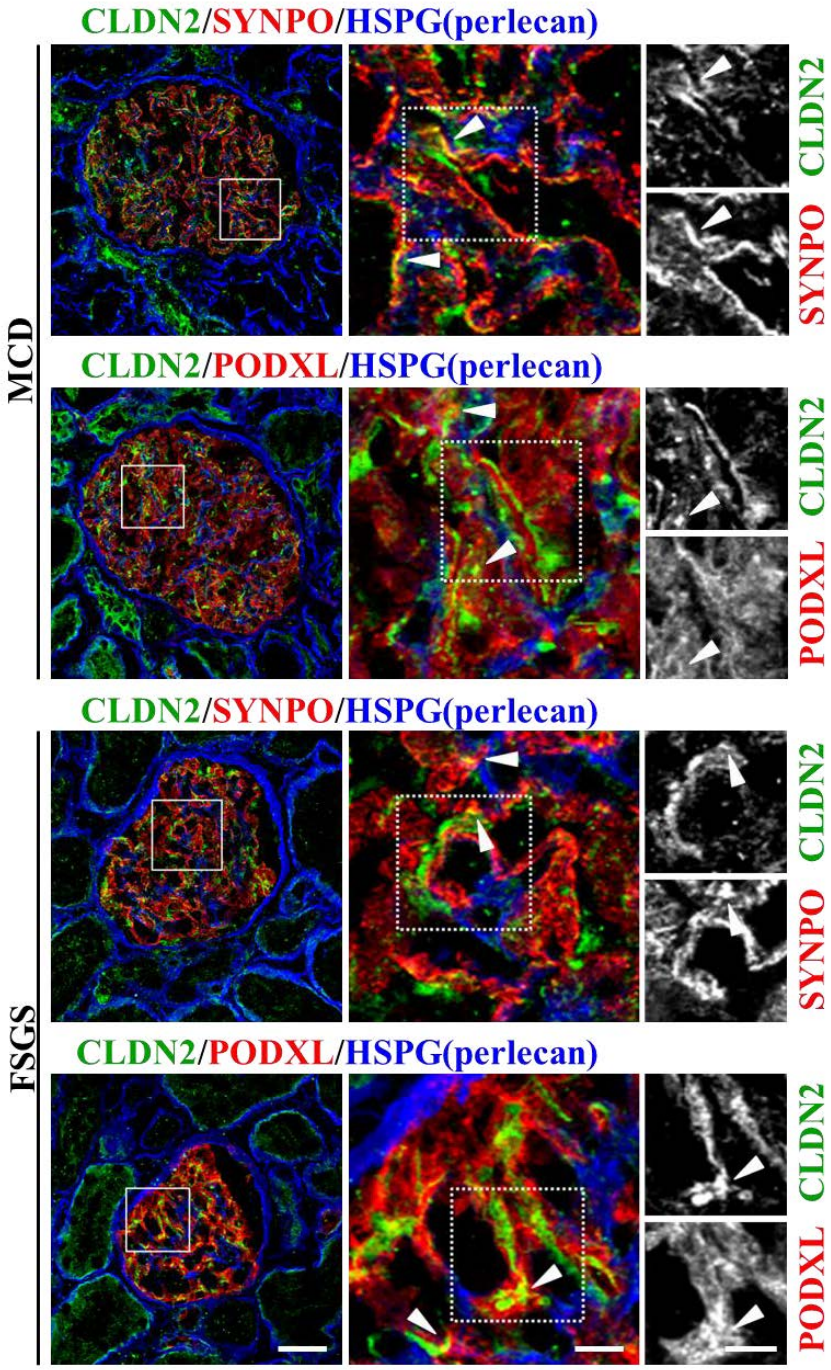

Figure 3: CLDN2 is at least partially colocalized with the podocyte markers synaptopodin (SYNPO) and podocalyxin (PODXL) in MCD and FSGS glomeruli before remission.

Renal biopsy sections were subjected to immunostaining with the corresponding antibodies. CLDN2 is stained green, SYNPO and PODXL are red, and HSPG (perlecan) is blue. Arrowheads indicate colocalization of CLDN2 with the podocyte markers. Bars; 50 μm in the left panel, 10 μm in the middle and right panels.

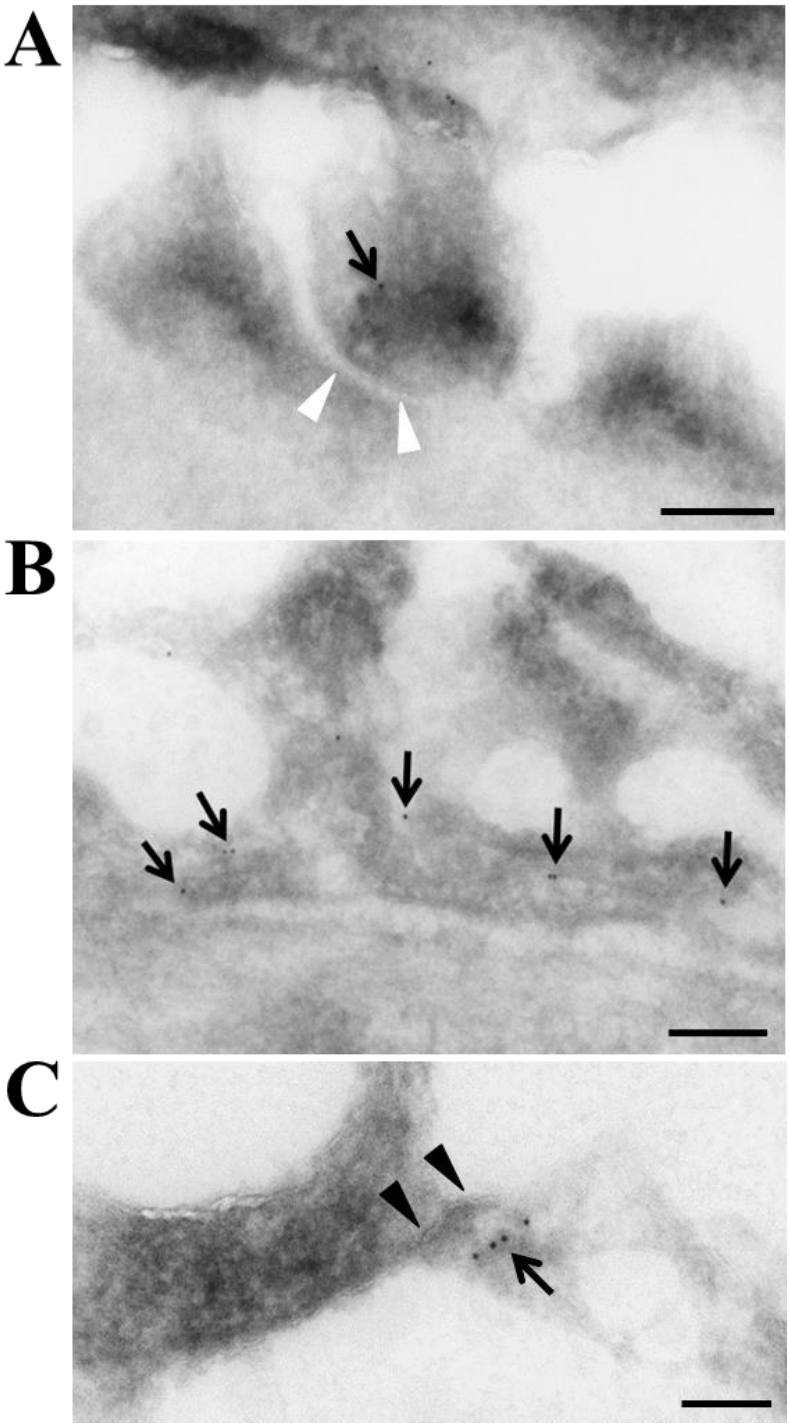

Figure 4: Immunogold electron micrographs showing the presence of CLDN2 in podocytes from MCD before remission.

White and black arrowheads indicate SDs and newly formed TJs, respectively. Arrows reveal the CLDN2 labeling in residual (A) and fused (B) foot processes, as well as at TJs (C). Bars; 200 nm.

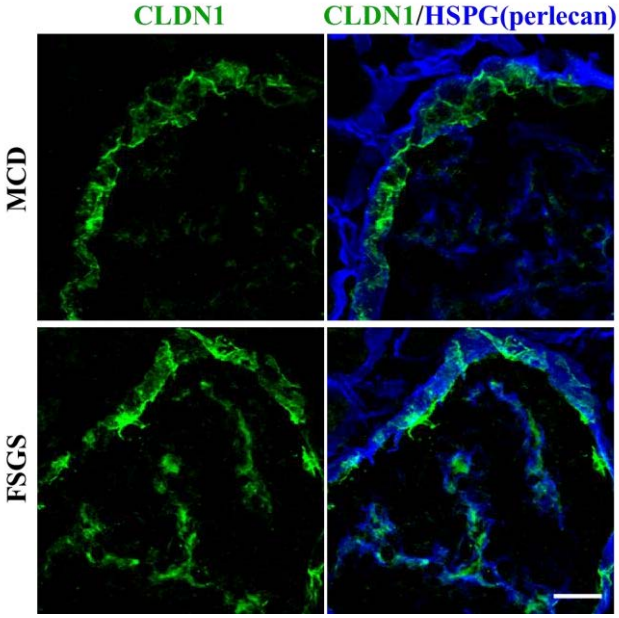

Figure 5: CLDN1 is segmentally observed in FSGS glomeruli but not in MCD glomeruli before remission.

Renal biopsy sections were subjected to immunostaining with the corresponding antibodies. CLDN1 is stained green and HSPG (perlecan) is blue. Bar, 25 μm.

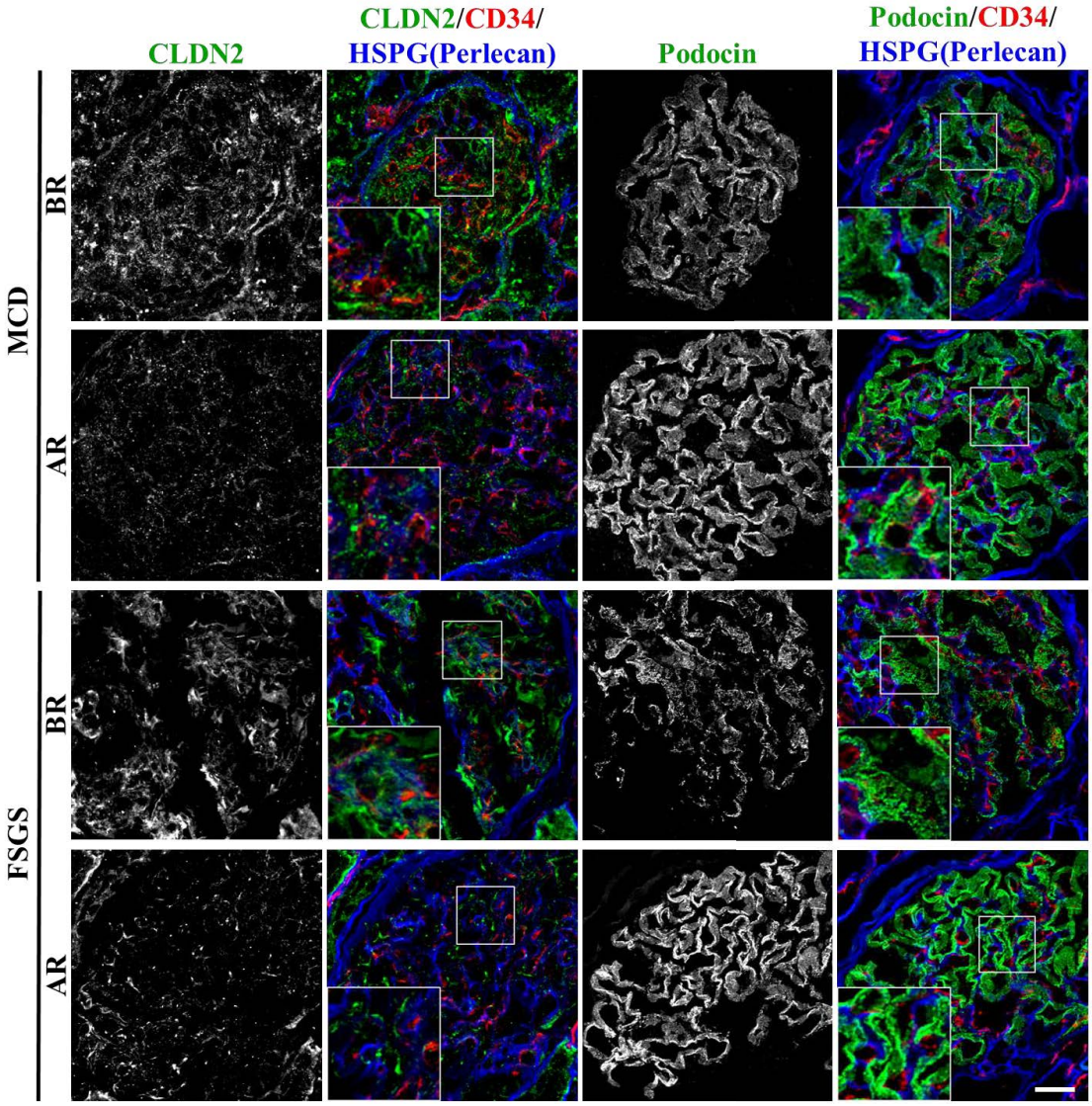

Figure 6: The strong filamentous signals for CLDN2 are appeared together with decrease of filamentous signals and change to the granulated pattern for podocin in MCD and FSGS glomeruli before remission.

Renal biopsy sections were subjected to immunostaining with the corresponding antibodies. Typical micrographs are shown for the before remission (BR) and after remission (AR) cases in MCD and FSGS. In the Merge panels, CLDN2 and podocin are stained green, CD34 is red and HSPG (perlecan) is blue. Bar, 25 μm.